Title
Design of coupled Andronov–Hopf oscillators with desired strange attractors

Journal
Nonlinear Dynamics, 100(2)

ISSN
0924-090X

Authors
Kohannim, Saba
Iwasaki, Tetsuya

Publication Date
2020-04-01

DOI
10.1007/s11071-020-05547-0

Peer reviewed

Noname manuscript No.
(will be inserted by the editor)

Design of Coupled Andronov-Hopf Oscillators with Desired Strange Attractors

Saba Kohannim* · **Tetsuya Iwasaki**

Received: date / Accepted: date

Abstract This paper develops a design method for the interconnections of a network of Andronov-Hopf oscillators such that the system exhibits a desired strange attractor. Because of the structure of the oscillators, the desired behavior can be achieved via weak linear coupling, which destabilizes the oscillators' phase difference. First, a set of sufficient conditions are established that result in phase destabilization, and thus instability, of a desired periodic solution. Then, an additional condition is determined to ensure that all harmonic periodic orbits will be unstable. Finally, additional numerical properties are assessed, where tuning of a small parameter can result in chaos.

Keywords Strange attractors · Chaos · Anti-control · Andronov-Hopf oscillators

1 Introduction

Evidence of strange attractors and chaos are prevalent in various biological systems, particularly in neural dynamics and cardiac rhythm. Chaotic regimes have been observed in the nervous system [1] and neural assemblies, and are known to promote adaptability and flexibility [2]. Strange attractors have also been found to be related to neuromuscular control of locomotion [3,4] and the ability to rapidly switch between various gaits available in the attractor [5]. Furthermore, various evidence suggests that the dynamics of brain waves

S. Kohannim
Department of Mechanical and Aersopace Engineering,
University of California, Los Angeles, Los Angeles
E-mail: sabakohannim@ucla.edu

T. Iwasaki
Department of Mechanical and Aersopace Engineering,
University of California, Los Angeles, Los Angeles
E-mail: tiwasaki@ucla.edu

are best described by strange nonchaotic attractors [6], which have fractal structures but are not sensitive to initial conditions.

Due to the observed benefits and potential applications, the problem of "anti-control", or forced generation of chaotic behavior, has received significant interest. However, little work has focused on the design of chaotic attractors with specified (unstable) limit cycles in the attractor, where chaos could potentially be exploited to stabilize the desired orbits through small control [7]. Moreover, most of the research has solely focused on discrete-time systems. In particular, Chen-Lai developed an algorithm for chaotification using linear state-feedback and mod-operations [8,9]. However, their methods cannot be modified or applied to continuous-time systems. Various schemes have been studied in the literature for the anti-control of continuous-time systems, including applying suitable control inputs to force the system to match a predesigned chaotic system [10,11]. Other works generate chaos via time-delayed feedback, but require simulation results and parameter tuning [12–15]. Most recently, [16] provided semi-analytical guidelines for designing a chaotic system. However, their method requires nonlinear control, and does not apply to systems where the necessary nonlinearity is embedded in the plant. Moreover, the final chaotic motion is not on a designed strange attractor. Thus, it remains open how to design a continuous-time system such that it possesses a strange attractor with desired limit cycles embedded in the attractor.

In this paper, we address this open problem and consider the case where the plant is a set of coupled oscillators. Due to their ability to capture complex dynamic behavior with a fairly simple structure, Andronov-Hopf oscillators are widely used to model networks of neurons in biological systems [17,18]. To this end, we choose a set of linearly coupled two-dimensional Andronov-Hopf oscillators, and find conditions on the interconnections that result in the existence of a strange attractor, with a desired limit cycle embedded in the attractor. First, we determine sufficient conditions to ensure the phase instability of a desired limit cycle, with a designable instability magnitude and direction. Then, we consider a special case of "pseudo-antisymmetric" weak coupling and determine sufficient conditions to guarantee that all harmonic periodic orbits are unstable. Finally, using numerical evidence, we consider several additional conditions that increase disorder and contribute to the transition from a strange nonchaotic attractor to a chaotic attractor. Preliminary results of this research were presented in [19].

The contents of this paper are organized as follows. In Section 2, we briefly review some mathematical definitions for various types of attractors and their essential quantitative tools. Section 3 is devoted to the description of the Andronov-Hopf oscillator model and the control objective. In Section 4, sufficient conditions for the instability of a designated orbit are found, followed by the development of additional specifications to ensure instability of all harmonic orbits in Section 5. Two numerical examples are then presented in Section 6 to demonstrate the effectiveness of the method. Finally, Section 7 concludes the main findings.

2 Preliminary definitions

Consider an autonomous nonlinear system

$$\dot{x} = f(x), \tag{1}$$

where $x(t) \in \mathbb{R}^n$. If the solution of the n-dimensional system approaches a set of states or points in phase space after transients die out, then that set is called an **attractor**. Classical types of attractors include stable equilibrium points, limit cycles, and quasi-periodic orbits. In the phase space, or the space whose coordinates are the state variables, these motions are associated with a fixed point, a closed curve, and a surface, respectively. It is also possible for an attractor in the phase space to be a **fractal set**: a set of points with a non-integer fractal dimension less than n. In that case, the attractor would be classified as strange. Hence, a **strange attractor** is an attractor with dimension $d < n$, where d is a non-integer [20]. In order to calculate the dimension of an attractor in an n-dimensional state space, we consider the Hausdorff dimension and the following definition.

Definition 1 *[21] Consider a set in an m-dimensional Euclidean space covered by m-dimensional cubes of edge length ϵ_i. Let*

$$l_d = \lim_{\epsilon \to 0} \inf \sum_i \epsilon_i^d, \qquad \textit{subject to} \qquad \epsilon_i \leq \epsilon,$$

where the infimum is taken over all feasible coverings. The Hausdorff dimension of the set is defined as the critical positive value of d, such that $l_c = 0$ if $c > d$ and $l_c = \infty$ if $c < d$.

It is reasonable to assume that all trajectories with initial conditions in the basin of an attractor will have the same **maximum Lyapunov exponent**, which measures the exponential attraction or separation rate of an infinitesimally perturbed trajectory [21]. In this paper, we consider the following definition.

Definition 2 *Suppose $\bar{x}(t)$ is a trajectory of the system (1). The maximum Lyapunov exponent, which measures the exponential attraction or separation in time of adjacent trajectories to $\bar{x}(t)$, is defined as follows. Let $\Phi(t) \in \mathbb{R}^{n\times n}$ be the fundamental matrix for the system linearized about $\bar{x}(t)$, given by*

$$\dot{\Phi}(t) = A(t)\Phi(t), \qquad \Phi(0) = I, \qquad A(t) := \frac{\partial f(\bar{x})}{\partial x}. \tag{2}$$

Define the maximum singular value of the fundamental matrix, $\sigma(t) = \bar{\sigma}(\Phi(t))$. Then, the maximum Lyapunov exponent of $\bar{x}(t)$ is defined as [22]

$$\lambda := \lim_{t\to\infty} \frac{1}{t} \ln \sigma(t).$$

An attractor is classified as **chaotic** when there exists a bounded solution $\bar{x}(t)$, with the initial condition on the basin of the attractor, such that $\lambda > 0$. This condition is valid for numerical analysis due to inaccuracies in numerical simulations, which prevent a trajectory from settling on an unstable limit cycle, even with exact initial conditions on the limit cycle. Hence, if one such solution $\bar{x}(t)$ is numerically found, then the corresponding attractor is chaotic. When $\bar{x}(t)$ is a known (or desired in the case of design) *analytical* solution of the system, $\lambda > 0$ is only a sufficient condition for $\bar{x}(t)$ being unstable. For instance, an exponentially unstable periodic solution $\bar{x}(t)$ has $\lambda > 0$, but its orbit is not an attractor and hence we do not classify it as chaotic. One may be tempted to conclude existence of a chaotic attractor by instability of a periodic orbit and boundedness of every nearby trajectories. However, this is clearly false because there may be a different stable limit cycle or equilibrium point nearby for the trajectory to settle to, in which case, λ is non-positive. This will be explored further in Section 4.

3 Problem formulation

Consider a network of n coupled two-dimensional Andronov-Hopf oscillators, given by

$$\dot{x} = \begin{bmatrix} \mathcal{E}(x) & -I \\ I & \mathcal{E}(x) \end{bmatrix} x + u(x), \tag{3}$$

$$x = \begin{bmatrix} q \\ p \end{bmatrix}, \qquad \begin{array}{l} \mathcal{E}(x) := \operatorname{diag}(a_1, \ldots, a_n), \\ a_i := 1 - (q_i^2 + p_i^2), \end{array}$$

where $x \in \mathbb{R}^{2n}$, and the coupling enters through the control input $u(x) \in \mathbb{R}^{2n}$. Without a coupling term, the system has the general periodic solution $x(t) = \xi(t)$ with

$$\xi(t) = \begin{bmatrix} C_\eta \mathring{\mathbf{1}} \\ S_\eta \mathring{\mathbf{1}} \end{bmatrix}, \qquad \eta := t\mathring{\mathbf{1}} + \varphi, \qquad \mathring{\mathbf{1}} := \operatorname{col}(1, ..., 1), \tag{4}$$

where $\varphi \in \mathbb{R}^n$ are arbitrary, and

$$C_z := \cos(\operatorname{diag}(z)), \qquad S_z := \sin(\operatorname{diag}(z)),$$

for an arbitrary vector z. Because the plant can be separated into a skew-symmetric section and a nonlinear section, coming from the $\mathcal{E}(x)$ term, $\xi(t)$ is amplitude and period locked at $\mathring{\mathbf{1}}$ and 2π seconds, respectively. However, the phase $\varphi \in \mathbb{R}^n$ remains arbitrary and a function of the initial conditions. Sinusoidal orbits with different amplitudes and frequencies can be considered, but these values are normalized here without loss of generality.

Our objective is to design the feedback control law $u(x)$ such that the system contains a strange attractor, with an unstable limit cycle embedded in the attractor. We assume that the target limit cycle, denoted by $\hat{\xi}(t)$, is given by (4) with a specific phase $\varphi = \hat{\varphi} \in \mathbb{R}^n$. Hypothetically, the controller would add weak coupling between the oscillators, such that the amplitudes remain bounded in the neighborhood of $\mathring{\mathbf{1}}$, while the phase dynamics destabilize so that the trajectory never settles at a stable harmonic limit cycle. It is well understood that fractal dynamics is only feasible in a nonlinear system. Since the plant, without controller input $u(x)$ is already nonlinear, it is possible to generate a strange attractor and achieve our goal using a linear controller, given by

$$u = \varepsilon H x. \tag{5}$$

With the form in (5), the controller represents the linear coupling between the oscillators. In order to maintain the stability of the oscillators' amplitudes, we only consider weak coupling, where the order of the coupling is denoted by a sufficiently small $\varepsilon > 0$.

Without coupling ($\varepsilon = 0$), condition $\mathcal{E}(x) = 0$ defines an invariant set as a group of n circular orbits on the (q_i, p_i) planes. With the weak coupling, smallness of $|\varepsilon|$ ensures existence of an invariant set in the neighborhood of the original invariant set.

Lemma 1 *Consider system (3) with (5). For each scalar $\delta \in (0,1/2)$, there exists $\bar{\varepsilon} > 0$ such that the set*

$$\mathbb{S}_\delta := \{\ x \in \mathbb{R}^{2n} :\ 1-\delta \le q_i^2 + p_i^2 \le 1+\delta,\ x = \mathrm{col}(q,p),\ i \in \mathbb{I}_n\ \},$$
$$\mathbb{I}_n := \{1, 2, \ldots, n\} \tag{6}$$

is invariant whenever $|\varepsilon| < \bar{\varepsilon}$. Moreover, the invariant set $\mathbb{S}_\delta$ is locally attractive in the sense that, given any nonzero initial state, not in $\mathbb{S}_\delta$, but in the neighborhood of $\mathbb{S}_\delta$, the trajectory $x(t)$ eventually enters $\mathbb{S}_\delta$.

Proof See Appendix.

A chaotic attractor may be embedded in the invariant set $\mathbb{S}_\delta$ if we ensure that there is no stable equilibrium nor periodic orbit in it. In the next section, we will develop a sufficiency condition on the weak coupling εH that analytically guarantees the instability of a particular periodic orbit $\hat{\xi}(t)$ that resides in $\mathbb{S}_\delta$. We will then formulate additional specifications to ensure the instability of all harmonic orbits in Section 5, and present numerical examples in Section 6.

4 Conditions for orbital instability

In the study of system stability, Lyapunov exponents are generally used to quantify a system's sensitivity to initial conditions via numerical simulations. In this paper, however, we will use the definition of the maximum Lyapunov exponent to analytically design the instability of a desired solution of the system.

4.1 General condition for positive Lyapunov exponent

Although the maximum Lyapunov exponent is a practical and effective tool in the numerical analysis of chaotic systems, it is difficult for use in analytical analysis. Thus, we consider an exponentially weighted fundamental matrix given by

$$\Psi(t) := e^{-\mu t}\Phi(t), \qquad \dot{\Psi}(t) = (A(t) - \mu I)\Psi(t), \qquad \Psi(0) = I, \tag{7}$$

for some constant $\mu \in \mathbb{R}$. Note that with Ψ, the maximum Lyapunov exponent is given by

$$\lambda = \mu + \lim_{t\to\infty} \frac{1}{t} \ln ||\Psi(t)||.$$

We now see that

$$\begin{aligned} \lambda < \mu \qquad &\Rightarrow \qquad \lim_{t\to\infty} ||\Psi(t)|| \to 0, \\ \lambda > \mu \qquad &\Rightarrow \qquad \lim_{t\to\infty} ||\Psi(t)|| \to \infty. \end{aligned}$$

Thus, a lower bound, useful for the coupling design, can now be derived from the following characterization of the maximum Lyapunov exponent:

$$\lambda = \sup \mu \qquad \text{subject to} \qquad \lim_{t\to\infty} ||\Psi(t)|| \to \infty. \tag{8}$$

Using this lower bound, as well as matrix norm and trace properties, we can formulate a sufficiency condition for the positivity of the maximum Lyapunov exponent. First, we prove a preliminary result in Lemma 2. To state the result, let $\mathbb{P}$ be the set of bounded, continuously differentiable, matrix-valued functions $P(t)$ such that $P(t) = P(t)^{\mathsf{T}} \geq 0$ and $P(t)$ is nonzero for all $t \geq 0$.

Lemma 2 *Let $\rho(t) \geq 0$ be a scalar function such that* $\mathrm{tr}(\Phi(t)^{\mathsf{T}} P(t)\Phi(t)) \geq \rho(t)$ *for some $P \in \mathbb{P}$. Consider the maximum Lyapunov exponent λ characterized in (8), and define $\tilde{\mu}$ as*

$$\tilde{\mu} := \sup \mu \qquad \textit{such that} \qquad \lim_{t\to\infty} e^{-2\mu t}\rho(t) \to \infty,$$

Then, it always holds that $\lambda \geq \tilde{\mu}$. Thus, $\tilde{\mu} > 0$ is a sufficient condition for $\lambda > 0$.

Proof See Appendix.

Using this Lemma, we can now determine a sufficient condition that ensures the positivity of the maximum Lyapunov exponent of a given trajectory $\bar{x}(t)$.

Lemma 3 *Consider a nonlinear system $\dot{x} = f(x)$ and an arbitrary solution $\bar{x}(t)$ defined for $t \geq 0$, where the linearized system about $\bar{x}(t)$ is given by (2). Suppose there exist a $P \in \mathbb{P}$, a scalar-valued function $\alpha(t) \in \mathbb{R}$, and scalars $t_1 \geq 0$ and $\epsilon > 0$, such that the following conditions are satisfied for all $t \geq t_1$:*

$$A(t)^{\mathsf{T}}P(t) + P(t)A(t) + \dot{P}(t) \geq \alpha(t)P(t), \qquad \int_{t_1}^{t} \alpha(\mathrm{t})d\mathrm{t} \geq \epsilon(t - t_1).$$

Then it is guaranteed that $\lambda \geq \epsilon/2$*, where* λ *is the maximum Lyapunov exponent of* $\bar{x}(t)$*.*

Proof We are going to prove this using the lower bound in Lemma 2 above. Using the dynamics,

$$\begin{aligned}\frac{d}{dt}\mathrm{tr}\Big(\Phi(t)^\intercal P(t)\Phi(t)\Big) &= \mathrm{tr}\Big(\Phi(t)^\intercal(A(t)^\intercal P(t)+P(t)A(t)+\dot{P}(t))\Phi(t)\Big),\\ &\geq \alpha(t)\ \mathrm{tr}\Big(\Phi(t)^\intercal P(t)\Phi(t)\Big)\end{aligned}$$

holds for all $t \geq 0$. Then, using a lower bound version of the Gronwall's inequality,

$$\mathrm{tr}\Big(\Phi(t)^\intercal P(t)\Phi(t)\Big) \geq e^{\int_0^t \alpha(t)dt}\ \mathrm{tr}\Big(P(0)\Big) =: \rho(t).$$

Now, for $\tilde{\mu} := \epsilon/2$ and an arbitrary $\delta > 0$, we have

$$e^{-2(\tilde{\mu}-\delta)t}\rho(t) \geq e^{(-\epsilon+2\delta)t}e^{\epsilon(t-t_1)}e^{\int_0^{t_1} \alpha(t)dt}\ \mathrm{tr}\Big(P(0)\Big) = e^{2\delta t}e^{-\epsilon t_1}\rho(t_1),$$

where the right hand side of the inequality goes to infinity as $t \to \infty$, and hence so does the left hand side. Therefore, from Lemma 2, we conclude that $\lambda \geq \epsilon/2$.

In the Lemma above, $\epsilon/2$ represents the lower bound of the magnitude of instability as measured by the maximum Lyapunov exponent for the trajectory $\bar{x}$. Furthermore, $P(t)$ contains information on the direction of the instability. We will now use this condition to design a controller $u(x)$ of the form in (5) to ensure that the target limit cycle $\hat{\xi}(t)$ of system (3) given by (4) with a specific phase $\varphi = \hat{\varphi}$ is unstable.

4.2 Coupling condition for instability of a desired orbit

In order to use the condition in Lemma 3, we first consider the system description in terms of the amplitude-phase (r, θ) coordinates, i.e., (19) in the appendix, and linearize the dynamics about the solution $(r, \theta) = (\mathring{\mathbf{1}}, \hat{\eta})$, corresponding to the target periodic orbit $\hat{\xi}(t)$. Define

$$\rho := r - \mathring{\mathbf{1}}, \qquad \vartheta := \theta - \hat{\eta}, \qquad \hat{\eta} := \mathring{\mathbf{1}}t + \hat{\varphi}.$$

Linearizing the system around the solution $(\mathring{\mathbf{1}}, \hat{\eta})$, we obtain

$$\dot{w} = A(t)w, \qquad w := \begin{bmatrix}\rho\\ \vartheta\end{bmatrix}, \tag{9}$$

where

$$A(t) := \begin{bmatrix}-2I & 0\\ 0 & 0\end{bmatrix} + \varepsilon\Omega_{t\mathring{\mathbf{1}}}^\intercal \hat{H}\Omega_{t\mathring{\mathbf{1}}}, \qquad \hat{H} := \Omega_{\hat{\varphi}}^\intercal H\Omega_{\hat{\varphi}}, \qquad \Omega_z(t) := \begin{bmatrix}C_z & -S_z\\ S_z & C_z\end{bmatrix}.$$

Since the choice of $(r,\theta) = (\mathring{\mathbf{1}}, \hat{\eta})$ is a solution of system (3) when $u(x) = 0$, the coupling has to vanish on the target orbit for $(\mathring{\mathbf{1}}, \hat{\eta})$ to remain a solution of the coupled system for all time t. In that case, $\hat{H}$ has to satisfy the following:

$$\hat{H}\mathring{\mathbf{1}}_1 = 0, \qquad \hat{H}\mathring{\mathbf{1}}_2 = 0, \tag{10}$$

where $\mathring{\mathbf{1}}_1 := \mathrm{col}(0, \mathring{\mathbf{1}})$ and $\mathring{\mathbf{1}}_2 := \mathrm{col}(\mathring{\mathbf{1}}, 0)$. For an orbit with different amplitudes and oscillation frequency, similar but slightly more complicated conditions can be derived for εH to force the orbit to be a solution of the system.

Using Lemma 3, we can now formulate simple sufficient conditions that ensure the instability of the limit cycle. This is summarized in the following theorem.

Theorem 1 *Consider system (3) with $u(x)$ in (5), where $H := \Omega_{\hat{\varphi}} \hat{H} \Omega_{\hat{\varphi}}^{\mathsf{T}}$ and $\varepsilon > 0$. Suppose, for some nonzero vector $v \in \mathbb{C}^n$ and a scalar $a \in \mathbb{C}$ with positive real part, the following conditions are satisfied:*

$$\begin{array}{lll} \hat{H}\mathring{\mathbf{1}}_1 = 0, & \hat{H}_{11}^{\mathsf{T}} v = av, & \hat{H}_{12}^{\mathsf{T}} v = 0, \\ \hat{H}\mathring{\mathbf{1}}_2 = 0, & \hat{H}_{22}^{\mathsf{T}} v = av, & \hat{H}_{21}^{\mathsf{T}} v = 0, \end{array} \qquad \hat{H} = \begin{bmatrix} \hat{H}_{11} & \hat{H}_{12} \\ \hat{H}_{21} & \hat{H}_{22} \end{bmatrix}. \tag{11}$$

Then, the limit cycle $\hat{\xi}(t)$ described by (4) with $\varphi = \hat{\varphi}$ is an unstable solution of the closed-loop system.

Proof Following the preceding development, we will show that $(r,\theta) = (\mathring{\mathbf{1}}, \hat{\eta})$ is an unstable solution of the transformed system (19). The first two conditions are the same as those in (10), which ensure that the signal $x = \hat{\xi}$ is a solution of the system. Define $\nu := \mathrm{col}(0, v)$, and set $P = \nu\nu^*$. Then, it can be shown that

$$A(t)^{\mathsf{T}} P + PA(t) \geq 2\varepsilon \Re(a) P.$$

According to Lemma 3, the above is a sufficient condition for $\lambda \geq \varepsilon \Re(a) > 0$. Therefore, the prescribed limit cycle will be an unstable solution of the system.

The conditions in Theorem 1 show that there exists a direction $\mathrm{col}(\rho, \vartheta) = \mathrm{col}(0, v)$ in which a nearby solution diverges exponentially away from the target orbit, with the rate of divergence bounded below by the real part of εa. While satisfying the conditions in Theorem 1 ensures the instability of the desired limit cycle, it does not guarantee that the limit cycle will be embedded in a strange attractor, and that the system will be chaotic. It is likely that the states will merely reach a different stable limit cycle. Thus, further conditions are needed to guarantee the instability of any other periodic orbit that is a solution of the system for a given coupling εH.

4.3 Coupling condition for instability of all harmonic orbits

Thus far, we have determined sufficient conditions that guaranteed the instability of a desired orbit with designable magnitude and direction of instability. We now need to find additional conditions on the interconnections between the oscillators that will generate a strange attractor. This is a very difficult problem, particularly since the trajectories in $\mathbb{S}_\delta$ are very sensitive to the smallest variations in coupling. As a necessary condition, we guarantee that the trajectory will not reach a different stable harmonic orbit. It turns out that a particular "pseudo-antisymmetric" form of the coupling matrix εH can greatly simplify analytical study of the system. However, numerical analyses indicate that this form usually lacks the disorderliness that leads to chaos, and breaking the structure is suitable for generating chaotic behavior. We now look at these results.

Consider the case where the coupling matrix H can be expressed as H_P with the following structure:

$$H_P = \begin{bmatrix} H_{11} & -H_{12} \\ H_{12} & H_{11} \end{bmatrix}. \tag{12}$$

We refer to matrices of this structure as pseudo-antisymmetric, which arise when representing a complex matrix by a real matrix of doubled dimensions, i.e. $H_P \in \mathbb{R}^{2n\times 2n}$ above is a representation of $H_{11} + jH_{12} \in \mathbb{C}^{n\times n}$. In this special case, linearizing about any general sinusoidal solution $(r,\theta) = (\gamma, \omega t + \varphi)$, for $(\gamma,\omega,\varphi) \in \mathbb{R}^n \times \mathbb{R}^n \times \mathbb{R}^n$, will result in (9) with a time-invariant Jacobian matrix A, given by

$$A = T^{-1}\mathsf{A}T, \qquad \mathsf{A} := \left(\begin{bmatrix} I - 3\Gamma^2 & -I + \mathcal{W} \\ I - \mathcal{W} & I - \Gamma^2 \end{bmatrix} + \varepsilon \Omega_\varphi^\intercal H \Omega_\varphi \right), \tag{13}$$

where

$$T := \mathrm{diag}(I, \Gamma), \qquad \Gamma := \mathrm{diag}(\gamma), \qquad \mathcal{W} := \mathrm{diag}(\omega).$$

Since A is time invariant and is related to A through a similarity transform, the stability of the limit cycle is equivalent to A having one eigenvalue at the origin, and the rest in the open left half plane.

Lemma 4 *Consider system (3) with $u(x)$ given by (5). Then, all possible sinusoidal solutions $x = \xi$, with constant frequencies, phases, and amplitudes, are of the form*

$$\xi(t) = \begin{bmatrix} C_\theta \gamma \\ S_\theta \gamma \end{bmatrix}, \qquad \theta := \omega t + \varphi. \tag{14}$$

Proof Suppose a solution is given of the form $x(t) = \mathrm{col}(q(t), p(t))$, where $q(t)$ and $p(t)$ are arbitrary sinusoidal functions with frequency ω. Define the vector $\hat{x}_i := \mathrm{col}(q_i e_i, p_i e_i)$, where e_i is the i^{th} column of the n dimensional identity matrix. Then, multiplying (3) by $\hat{x}_i^\intercal$ from the left gives

$$\frac{1}{2}\frac{d}{dt}(p_i^2 + q_i^2) = p_i^2 + q_i^2 - (p_i^2 + q_i^2)^2 + \hat{x}_i^\intercal H x.$$

If $(q_i^2 + p_i^2)$ is not equal to a constant, but is a sinusoidal function with frequency 2ω, then the right hand side will have a harmonic term with frequency 4ω coming from the $(p_i^2 + q_i^2)^2$ term. However, this term cannot cancel any term from the left side, resulting in an inconsistency.

Lemma 5 *Consider system (3) with $u(x)$ given by (5) and H having the form in (12). Then for sufficiently small $|\varepsilon|$, the closed-loop system has infinitely many harmonic solutions of the form (14), all of them have amplitudes γ close to $\mathring{\mathbf{1}}$ or 0, and those in the neighborhood of $\gamma = \mathring{\mathbf{1}}$ can be parametrized as $x = \xi$ with (14) and*

$$\begin{array}{l} \gamma = \mathring{\mathbf{1}} + (\varepsilon/2)\bar{H}_{11}\mathring{\mathbf{1}} + \mathcal{O}(\varepsilon^2), \\ \omega = \mathring{\mathbf{1}} + \varepsilon\bar{H}_{21}\mathring{\mathbf{1}} + \mathcal{O}(\varepsilon^2), \end{array} \qquad \begin{bmatrix} \bar{H}_{11} & \bar{H}_{12} \\ \bar{H}_{21} & \bar{H}_{22} \end{bmatrix} := \Omega_\varphi^\mathsf{T} H \Omega_\varphi, \tag{15}$$

where $\varphi \in \mathbb{R}^n$ is arbitrary.

Proof See Appendix.

Theorem 2 *Consider the linear system $\dot{\mathsf{w}} = \mathsf{A}\mathsf{w}$ with A in (13), where $\varepsilon \in \mathbb{R}$, $\varphi \in \mathbb{R}^n$, and $H \in \mathbb{R}^{2n\times 2n}$ are given, and $\gamma, \omega \in \mathbb{R}^n$ are specified in (15). Suppose H has the structure in (12) and*

$$\mathrm{tr}(H) > 2\mathsf{x}^\mathsf{T} H \mathsf{x} \qquad \mathsf{x} := \begin{bmatrix} \cos\varphi \\ \sin\varphi \end{bmatrix} \in \mathbb{R}^{2n}. \tag{16}$$

Then A has at least one eigenvalue with a positive real part when $|\varepsilon|$ is sufficiently small.

Proof First note that, if we neglect the $\mathcal{O}(\varepsilon^2)$ terms, A can be represented by

$$\mathsf{A} = \begin{bmatrix} \mathsf{A}_{11} & \varepsilon\mathsf{A}_{12} \\ -\varepsilon\mathsf{A}_{21} & \varepsilon\mathsf{A}_{22} \end{bmatrix} := \begin{bmatrix} -2I & 0 \\ 0 & 0 \end{bmatrix} + \varepsilon \begin{bmatrix} \bar{H}_{11} - 3\tilde{H}_1 & \bar{H}_{12} + \tilde{H}_2 \\ \bar{H}_{21} - \tilde{H}_2 & \bar{H}_{22} - \tilde{H}_1 \end{bmatrix},$$

$$\begin{array}{l} \tilde{H}_1 := \mathrm{diag}(\bar{H}_{11}\mathring{\mathbf{1}}), \\ \tilde{H}_2 := \mathrm{diag}(\bar{H}_{21}\mathring{\mathbf{1}}). \end{array}$$

When $\varepsilon = 0$, matrix A has n eigenvalues at -2 and the other n eigenvalues at the origin. By continuity, the eigenvalues remain in the neighborhood of -2 and 0 for small $|\varepsilon|$. Let an eigenvalue near 0 be denoted as λ_ε. Then, using the determinant formula,

$$\det(\lambda_\varepsilon I - \mathsf{A}) = \det(\lambda_\varepsilon I - \mathsf{A}_{11})\det(\lambda_\varepsilon I - \varepsilon\mathsf{A}_{22} + \varepsilon^2\mathsf{A}_{21}(\lambda_\varepsilon I - \mathsf{A}_{11})^{-1}\mathsf{A}_{12}) = 0,$$

which shows that $\lambda_\varepsilon/\varepsilon$ approaches an eigenvalue of A_{22} as $|\varepsilon|$ approaches zero. Thus, for small enough ε, the eigenvalues of A can be approximated by the eigenvalues of A_{11} and $\varepsilon\mathsf{A}_{22}$. Then, $\mathrm{tr}(\mathsf{A}_{22}) > 0$ is a sufficient condition for A having an eigenvalue in the right half plane. Using simple trace properties and the structure of H, it can be verified that

$$\mathrm{tr}(\mathsf{A}_{22}) = \mathrm{tr}\Big(H(I/2 - \mathsf{x}\mathsf{x}^\mathsf{T})\Big),$$

and thus $\mathrm{tr}(\mathsf{A}_{22}) > 0$ is equivalent to (16).

5 Controller design for generating a strange attractor

5.1 Pseudo-antisymmetric coupling design

We now use the technical tools developed in the previous sections to design the coupling matrix H to embed an attractor in the state space. The idea is to make $\mathbb{S}_\delta$ in Lemma 1 an attractor by weak coupling (i.e. small $\varepsilon > 0$), embed a particular unstable limit cycle, $\hat{\xi}(t)$ described by (4) with $\varphi = \hat{\varphi}$, in the attractor by choosing the structure of coupling H as in Theorem 1, and ensure that none of the possible harmonic limit cycles is stable by requiring (16) in Theorem 2 for all $\varphi \in \mathbb{R}^n$. It turns out, however, that the trace condition (16) is too conservative to capture instability of all possible harmonic solutions. In particular, if H has been chosen to satisfy the properties in Theorem 1, then $\hat{x} := \mathrm{col}(\cos\hat{\varphi}, \sin\hat{\varphi})$ corresponding to the unstable solution $\hat{\xi}(t)$ is often found not to satisfy the sufficient (conservative) condition in (16). Therefore, we enforce the instability condition (16) for all φ except for those in the neighborhood of $\hat{\varphi}$, with the expectation that stable harmonic solutions do not exist in the neighborhood of $\hat{\xi}$ due to its instability.

We will now summarize the conditions on εH that guarantee the the properties described above in the following theorem.

Theorem 3 *Consider system (3) with $u(x)$ given by (5), where the coupling matrix H has the structure in (12) and satisfies the conditions in Theorem 1 for some $\hat{\varphi}$. Suppose general multipliers $\tau_i(\mathsf{x}) \in \mathbb{R}$ and $\varrho(\mathsf{x}) \geq 0$ exist such that the following condition is satisfied:*

$$\mathrm{tr}(H) - 2\mathsf{x}^\intercal H \mathsf{x} > \sum_{i=1}^{n} \tau_i(\mathsf{x})(1 - \mathsf{x}^\intercal Q_i \mathsf{x}) + \varrho(\mathsf{x})(\|\mathsf{x} - \hat{\mathsf{x}}\|^2 - \hbar^2), \qquad \forall\ \mathsf{x} \in \mathbb{R}^{2n}, \tag{17}$$

where $\hat{\mathsf{x}} := \mathrm{col}(\cos\hat{\varphi}, \sin\hat{\varphi})$, $Q_i := \mathrm{diag}(e_i e_i^\intercal, e_i e_i^\intercal)$, $e_i \in \mathbb{R}^n$ is the i^{th} column of the $n \times n$ identity matrix, and $\hbar \in \mathbb{R}$ is a given positive number. Then, for a small enough ε, the set $\mathbb{S}_\delta$ in (6) with $\delta \in (0, 1/2)$ is invariant and attractive, and no trajectory of system (3), starting from the basin of attraction, will converge to a stable sinusoidal solution of the form in (14) with phase φ satisfying $\|\mathsf{x} - \hat{\mathsf{x}}\| > \hbar$. Moreover, $\hat{\xi}(t)$ described by (4) with $\varphi = \hat{\varphi}$ is an unstable limit cycle embedded in $\mathbb{S}_\delta$..

Proof According to Theorem 1, the limit cycle $\hat{\xi}(t)$ is already known to be an unstable solution of the system. Other possible sinusoidal solutions of the form in (14) are stable only if all the eigenvalues of A are in the closed left half plane. Based on Theorem 2, for small enough ε, satisfying (16) is a sufficient condition that A will have an eigenvalue in the right half plane for any sinusoidal solution that resides in $\mathbb{S}_\delta$. This condition is enforced for all such solutions with the phase φ satisfying $\|\mathsf{x} - \hat{\mathsf{x}}\| > \hbar$, where x is defined in (16), by the following statement:

$$\operatorname{tr}(H) > 2\mathsf{x}^\mathsf{T} H \mathsf{x} \qquad \forall\, \mathsf{x} \in \mathbb{R}^{2n} \qquad \text{such that} \qquad \begin{array}{l} \mathsf{x}^\mathsf{T} Q_i \mathsf{x} = 1, \\ \|\mathsf{x}-\hat{\mathsf{x}}\|^2 > \hbar^2, \qquad i \in \mathbb{I}_n, \end{array}$$

Finally, the S-procedure [23] is used to convert the above to one sufficient condition using multipliers τ_i and ϱ that possibly depend on x.

We can now use the specifications in Theorem 3 to find a coupling matrix εH that guarantees the instability of a desired limit cycle with a designable instability magnitude and direction specified by a and v in Theorem 1, as well as the nonexistence of any other stable sinusoidal solution with $\|\mathsf{x}-\hat{\mathsf{x}}\| > \hbar$ in the attractive invariant set $\mathbb{S}_\delta$. It is possible that a stable harmonic solution satisfying $\|\mathsf{x}-\hat{\mathsf{x}}\| \le \hbar$ exists, but the chance would be thin if $\hbar > 0$ is chosen to be small, due to instability of $\hat{\xi}$. We may then expect that every solution attracted into $\mathbb{S}_\delta$ has to wander around. A remaining possibility is convergence to a non-sinusoidal periodic orbit. We will examine the effectiveness of the condition in Theorem 3 through a numerical study later.

The design problem is reduced to the search for H, $\tau_i(\hat{\mathsf{x}})$, and $\varrho(\mathsf{x})$ satisfying (11) and (17), where the specifications are given by $(a, v, \hat{\varphi}) \in \mathbb{C} \times \mathbb{C}^n \times \mathbb{R}^n$ and $\hbar \in \mathbb{R}$. The conditions in (11) are linear and easy to solve numerically. With $\tau_i(\mathsf{x})$ and $\varrho(\mathsf{x})$ parametrized as polynomial functions, the overall feasibility problem, with constraints (11) and (17), can be formulated with SOSTOOLS, a free MATLAB toolbox for formatting sum of squares optimization problems. The problem was then solved using SeDuMi, a program that solves optimizations over linear, quadratic, and semidefinite constraints. For the examples given in Section 6, $\varrho(\mathsf{x})$ was a constant, and $\tau_i(\mathsf{x})$ was set to $\mathsf{t}_i + \mathsf{x}^\mathsf{T} \mathsf{T}_i \mathsf{x}$ for $\mathsf{t}_i \in \mathbb{R}$ and diagonal $\mathsf{T}_i \in \mathbb{R}^{2n \times 2n}$ as free parameters.

5.2 Pseudo-antisymmetry breaking and additional conditions for chaos generation

In the previous sections we determined specifications on the coupling εH such that (almost) no stable sinusoidal orbit was a solution of the system within $\mathbb{S}_\delta$. However, these conditions are not sufficient for chaos generation, as they do not eliminate the existence of strange nonchaotic attractors. In particular, when H has the pseudo-antisymmetric form of H_P, it could create undesired order amongst the oscillators. Based on considerable numerical examples, we speculate that pseudo-antisymmetry breaking is significant for increased disorder.

To maintain the specifications in Theorem 3 that have been satisfied, we break the structure through a small perturbation by choosing the following form for the coupling matrix H:

$$H = \Omega_{\hat{\varphi}} \begin{bmatrix} \hat{H}_{11} & (-1+\mathsf{e})\hat{H}_{12} \\ (1+\mathsf{e})\hat{H}_{12} & \hat{H}_{11} \end{bmatrix} \Omega_{\hat{\varphi}}^\mathsf{T}, \tag{18}$$

where $\mathtt{e}$ is a small scalar, and the conditions in (11) and (17) have been satisfied for $\mathtt{e} = 0$. It is clear that for any value of $\mathtt{e}$, the specifications in (11) still hold and the target oscillation $\xi(t)$ in (4) with $\varphi = \hat{\varphi}$ remains to be an unstable solution of the perturbed system. On the other hand, this is not necessarily true for the other condition (17). In fact, most of the harmonic oscillations characterized in (15) will no longer be solutions and may become distorted (non-sinusoidal) periodic orbits after the perturbation. However, we make the following conjecture: *Consider system (3) with $u(x)$ given by (5) and H given by (18). Suppose the coupling εH with $\mathtt{e} = 0$ satisfies the conditions in Theorem 3. Then for sufficiently small $|\mathtt{e}|$, all possible periodic solutions of system (3) will remain unstable.* The argument behind this conjecture is as follows. Assume that each sinusoidal solution $(\gamma, \omega t + \varphi)$ in (15) remains to be a periodic solution of the perturbed system with a slight orbital deformation $\mathcal{O}(\mathtt{e})$. Linearizing the oscillator model, with the above H in (18), about such periodic solution results in a Jacobian matrix equal to the summation of A in (13) plus a time-varying $\mathcal{O}(\mathtt{e})$ term. We reason that for small enough $\mathtt{e}$, the Jacobian matrix will remain close to the time-invariant component and the linearized system will remain unstable.

Although the variation of the coupling matrix with a nonzero $\mathtt{e}$ can increase disorder, it is still not a sufficient condition for the existence of a chaotic strange attractor. Unfortunately, determining an analytical sufficiency condition for chaos generation, without the need for numerical simulations and tuning, is extremely difficult. It is especially challenging when the controller is linear and does not contain particular nonlinearities, such as nonlinear delay feedback or sawtooth functions. Hence, we progress this study by finding additional properties that are generally satisfied in chaotic numerical examples, and can be formulated as analytical conditions on the controller.

Chaotic systems generally have positive and negative Lyapunov exponents. While the positive Lyapunov exponent indicates sensitivity to initial conditions, the negative exponent indicates that the trajectory returns to a previous vicinity, resulting in a stable strange attractor. In our system, we expect that with weak coupling, all n amplitude states of a generalcoffee hard candy trajectory will remain stable and lead to n negative Lyapunov exponents. However, we want one Lyapunov exponent, corresponding to the oscillators' phases, to be positive, one to be zero, and for all others to be negative. Numerical evidence indicates that this is more achievable when the trajectories in the strange attractor continuously approach and leave the vicinity of the desired unstable orbit $\hat{\xi}(t)$. Thus, we hypothesize that the time-invariant Jacobian A matrix, linearized about $\hat{\xi}(t)$ in (9) with pseudo-antisymmetric H, should have only one eigenvalue in the right half plane, one at the origin, and all others on the open left half plane. Based on the proof of Theorem 2, n eigenvalues of A associated with the amplitude ρ are close to -2, and the other n eigenvalues associated with the phase ϑ are approximately equal to the eigenvalues of $\varepsilon \hat{H}_{11}$. As a result, $\hat{H}_{11}$ should have only one positive eigenvalue. This can be converted to a restriction on the trace of the coupling matrix H. Furthermore, numerical case studies have indicated that it is easier to generate chaos when the trace of $\hat{H}_{12}$ has a larger absolute value. These properties can be included as additional linear conditions to be satisfied in the search for H.

6 Numerical examples

Example 1:

In this example, we consider a set of three coupled Andronov-Hopf oscillators, with their dynamics described by (3). We first find a numerical coupling matrix εH, with the pseudo-antisymmetric form in (12), that satisfies the conditions in Theorem 3, as well as the additional conditions from Section 5.2, for the following specifications:

$$\hat{\varphi} = \mathrm{col}(0, \pi/2, \pi), \qquad \varepsilon a = 0.1, \qquad v = \mathrm{col}(1, -2, 1), \qquad \hbar^2 = 0.005.$$

Using the form in (18), the following possible interconnection matrix εH is found:

$$\varepsilon H := \varepsilon \Omega_{\hat{\varphi}} \hat{H} \Omega_{\hat{\varphi}}^{\mathsf{T}},$$

where

$$\varepsilon \hat{H}_{11} = \begin{bmatrix} -0.2060 & 0.1706 & 0.0353 \\ -0.1706 & 0.2000 & -0.0294 \\ -0.0353 & 0.0294 & 0.0060 \end{bmatrix}, \quad \varepsilon \hat{H}_{12} = \begin{bmatrix} -0.1475 & 0.0000 & 0.1475 \\ 0.0000 & -0.0000 & -0.0000 \\ 0.1475 & -0.0000 & -0.1475 \end{bmatrix}.$$

The associated eigenvalues are given by

$$\begin{aligned} &\mathrm{eig}(\varepsilon \hat{H}_{11}) = (0.1, 0, -0.1), \\ &\mathrm{eig}(\varepsilon H) = (0.1, 0.1, 0, 0, -0.1000 \pm 0.2950j) \text{ for } \mathsf{e} = 0, \\ &\mathrm{eig}(A) = (0.1, 0, -0.1445, -1.9000, -2.0555, -2.0000) \end{aligned}$$

where A is the system matrix in (9) for the linearization around $(r, \theta) = (\mathring{\mathbf{1}}, \mathring{\mathbf{1}}t + \hat{\varphi})$. Note that because of the structure of H, all its eigenvalues are either repeated or complex conjugates. Furthermore, there is only one pair of positive eigenvalues. One eigenvalue of the pair corresponds to the desired a value, while the other becomes a negative eigenvalue of the Jacobian A matrix due to the $-2I$ term. This also occurs with the other pairs of eigenvalues, such that A will contain one positive eigenvalue, one zero eigenvalue, and all others in the open left half plane.

Figure 1 shows the results of the system simulation for $\mathsf{e} = 0$, with the initial conditions close to the desired unstable orbit. As expected, the trajectory never settles at a stable harmonic limit cycle. This is shown in Figure 1a, which is the phase portrait of the q states, with the red orbit indicating $(r, \theta) = (\mathring{\mathbf{1}}, \mathring{\mathbf{1}}t + \hat{\varphi})$. A Poincaré map of the q phase portrait is seen in Figure 1b, with the Poincaré section shown in green in Figure 1a. The Poincaré map consists of highly organized points in tight parallel lines that almost form a closed curve. Based on numerical computation, the map has a non-integer Hausdorff dimension

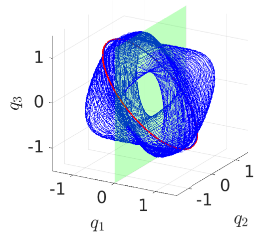

(a) Phase portrait of the oscillator's q states

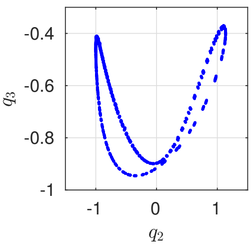

(b) A Poincaré map of Fig. 1a

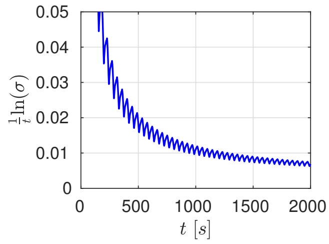

(c) Plot of the maximum Lyapunov exponent as $t \to \infty$

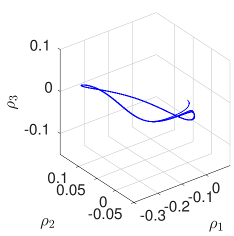

(d) Phase portrait of ρ

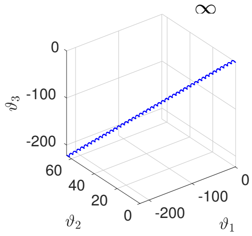

(e) Phase portrait of ϑ

Fig. 1: Simulation results for $\mathsf{e} = 0$

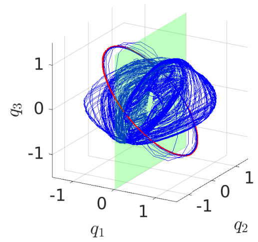

(a) Phase portrait of the oscillator's q states

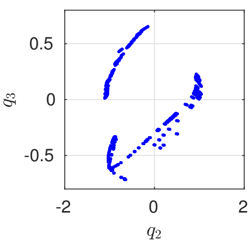

(b) A Poincaré map of Fig. 2a

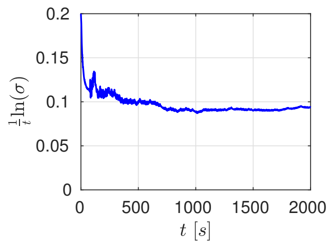

(c) Plot of the maximum Lyapunov exponent as $t \to \infty$

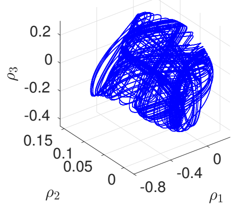

(d) Phase portrait of ρ

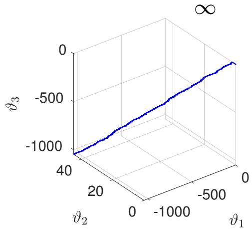

(e) Phase portrait of ϑ

Fig. 2: Simulation results for $\mathsf{e} = -2$

$d \approx 1.3$. Due to the map's appearance and fractal dimension, this signifies that the attractor is indeed strange [24]. In order to determine whether the strange attractor is chaotic, we look at the maximum Lyapunov exponent, or the limit of the plot in Figure 1c. Since the maximum Lyapunov exponent is approaching 0.003, indicating a rather slow exponential divergence, the strange attractor is indeed chaotic. Figures 1d and 1e show the phase portraits of ρ and ϑ, where $\rho := r - \mathring{\mathbf{1}}$, and $\vartheta := \theta - (\mathring{\mathbf{1}}t + \hat{\varphi})$. As expected, ρ is bounded and remains close to 0, while ϑ is unbounded and diverging away from the initial point close to the origin.

Figure 2 shows the simulation results when symmetry is broken by setting $\mathsf{e} = -2$. The symmetry breaking increases the disorder such that the trajectory becomes more chaotic and sensitive to initial conditions. In this case, the maximum Lyapunov exponent, the limit of the plot in Figure 2c, is approximately 0.08. The Poincaré map shown in Fig. 2b no longer makes a closed-curve, and the complexity in the phase portrait of ρ in Fig. 2d is substantially increased. Here, the value of e has been chosen large in comparison with 1, making H significantly deviate from the pseudo-antisymmetric structure. In this case, the analytical result in Theorem 3 does not apply, but simulations with various values of the scalar parameter e have revealed a variety of attractors. Thus, the additional freedom in the parameter e appears beneficial for creating chaotic attractors.

Example 2:

In this example, we begin with four Andronov-Hopf oscillator that are initially coupled with a coupling matrix εH^o to have a stable limit cycle $(r, \theta) = (\mathring{\mathbf{1}}, \mathring{\mathbf{1}}t)$ on which the oscillators are synchronized (i.e., $\hat{\varphi} = 0$). We then design a new coupling matrix, εH^f, following the same steps as the previous example, in order to destabilize the synchronized limit cycle and achieve chaos. This example illustrates a scenario where pathological synchronized neural activities are broken and healthy chaotic activities are recovered. For illustrative purposes, we make each Andronov-Hopf oscillator represent a neuron, and introduce output variables $v_i(t)$, representing the neuronal membrane potentials, as follows:

$$v_i(t) := \sum_{k=1}^{m} \Re\left[c_k \left(\frac{z_i(t)}{|z_i(t)|}\right)^k\right], \qquad z_i := x_i + jx_{i+3}, \qquad i = 1, \ldots, 4,$$

where $c_k \in \mathbb{C}$ are the Fourier coefficients of the action potential generated by the Hodgkin-Huxley neuron model [25] (i.e., the sum of $c_k e^{jk\omega t}$ is the Fourier series of the unbiased action potential), and $m = 50$ is the number of terms. (The time unit here is arbitrary and not adjusted to reflect the time scale of neural activities.)

Our initial coupling matrix εH^o, with a stable limit cycle at $(r,\theta) = (\mathring{\mathbf{1}}, \mathring{\mathbf{1}}t)$, is given by

$$\varepsilon H^o := \varepsilon \cdot \mathrm{diag}(\hat{H}_{11}^o, \hat{H}_{11}^o), \quad \varepsilon \hat{H}_{11}^o = \begin{bmatrix} -0.0151 & 0.0060 & 0.0045 & 0.0045 \\ 0.0060 & -0.0151 & 0.0045 & 0.0045 \\ 0.0118 & 0.0118 & -0.0385 & 0.0148 \\ 0.0118 & 0.0118 & 0.0148 & -0.0385 \end{bmatrix}.$$

We then find a new coupling matrix εH^f, with the pseudo-antisymmetric form in (12), that satisfies the conditions in Theorem 3, as well as the additional conditions from Section 5.2, for the following specifications:

$$\varepsilon a = 0.05, \qquad v = \mathrm{col}(1,0,-2,1), \qquad \hbar^2 = 0.005.$$

Using the form in (18), with $\mathsf{e} = 3$ and $\hat{\varphi} = 0$, the following possible interconnection matrix εH^f is found:

$$\varepsilon H^f := \varepsilon \begin{bmatrix} \hat{H}_{11}^f & 2\hat{H}_{12}^f \\ 4\hat{H}_{12}^f & \hat{H}_{11}^f \end{bmatrix},$$

$$\varepsilon \hat{H}_{11}^f = \begin{bmatrix} -0.0110 & -0.0071 & 0.0264 & -0.0083 \\ 0.0071 & -0.0289 & 0.0096 & 0.0121 \\ -0.0264 & -0.0096 & 0.0904 & -0.0544 \\ 0.0082 & -0.0121 & 0.0544 & -0.0505 \end{bmatrix},$$

$$\varepsilon \hat{H}_{12}^f = \begin{bmatrix} -0.0560 & 0.0370 & -0.0123 & 0.0314 \\ 0.0370 & -0.0391 & 0.0130 & -0.0109 \\ -0.0123 & 0.0130 & -0.0043 & 0.0036 \\ 0.0314 & -0.0109 & 0.0036 & -0.0241 \end{bmatrix}.$$

Figure 3 shows results of the system simulation when the coupling matrix is switched from εH^o to εH^f at $t = 300\ s$. Initially, the trajectory settles at the stable harmonic limit cycle on which the action potentials $v_i(t)$ synchronize (Figure 3a, top), and the maximum Lyapunov exponent, or the limit of the plot in Figure 3b, approaches zero. When the coupling matrix is changed to εH^f, the limit cycle is destabilized and the trajectory becomes chaotic. This is seen by looking at the maximum Lyapunov exponent, or the limit of the plot in Figure 3c, which jumps from zero and reaches above 0.006, indicating an exponential divergence. The spiking activities (Figure 3a, bottom) show a chaotic behavior where the trajectory occasionally returns to, and goes away from, the neighborhood of the synchronized state.

7 Conclusion

In this paper, we considered a set of two dimensional Andronov-Hopf oscillators, where the internal structure, without coupling, stabilizes the oscillators'

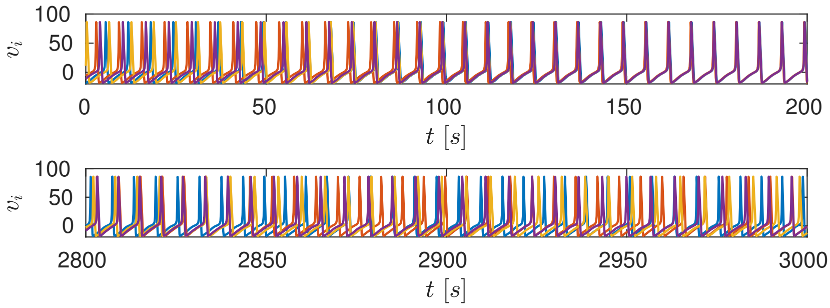

(a) Plots of the spiking outputs $v_i(t)$ for time durations $0 < t < 200$ and $2800 < t < 3000$

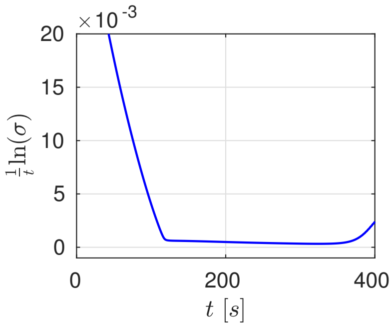

(b) Plot of the maximum Lyapunov exponent for time duration $0 < t < 400$

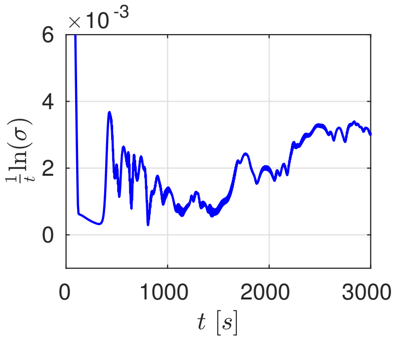

(c) Plot of the maximum Lyapunov exponent for time duration $0 < t < 3000$

Fig. 3: Simulation results showing transition from a stable limit cycle to chaos

frequency and amplitude. We then set out to design weak, linear interconnections between the oscillators such that the system dynamics would characterize a strange attractor, with a desired unstable orbit embedded in the attractor.

The first main contributions of this paper was developing simple eigenvalue/eigenvector conditions on the coupling matrix that forced a desired harmonic orbit to be an unstable solution of the system with a specified magnitude and direction of instability. The second main contribution was determining a specific pseudo-antisymmetric structure for the coupling matrix that greatly simplified system analysis. Specifically, with the particular pseudo-antisymmetric coupling, linearizing the system about all simple harmonic solutions resulted in a time-invariant Jacobian matrix. Using this property and the S-procedure, we developed a condition that ensured no harmonic orbit would be a stable solution of the system. Finally, using numerical analyses of chaotic systems, we determined several additional factors that we hypothesize can assist in stabilizing a strange attractor and increasing disorder and sensitivity to initial conditions.

Our numerical examples demonstrated that satisfying the conditions can lead to a system which generates the desired behavior; however, differentiating between a chaotic and nonchaotic strange attractor may require parameter tuning. Although the work of this study did not conclude with a completed sufficiency condition that solved the objective, we believe our results have set the groundwork for such a solution.

Appendix

Proof of Lemma 1:

Proof Consider the following coordinate transformation $(q,p) \leftrightarrow (r,\theta)$, defined by

$$q = C_\theta r, \qquad p = S_\theta r.$$

With the new state variables (r,θ), system (3) with coupling (5) can be expressed as

$$\begin{bmatrix} \dot{r} \\ R\dot{\theta} \end{bmatrix} = \begin{bmatrix} I - R^2 \\ I \end{bmatrix} r + \varepsilon \begin{bmatrix} C_\theta & S_\theta \\ -S_\theta & C_\theta \end{bmatrix} H \begin{bmatrix} C_\theta \\ S_\theta \end{bmatrix} r, \tag{19}$$

where $R := \mathrm{diag}(r)$. Let $x(t)$, $t \geq 0$, be an arbitrary trajectory starting at a point in $\mathbb{S}_\delta$. Suppose $x(t)$ hits the boundary of $\mathbb{S}_\delta$ at $t = t_1 \geq 0$ for the first time. Then there exists a subset of $\mathbb{I}_n$, denoted by $\mathbb{I}_{\mathrm{hit}}$, such that $r_k(t_1)^2 = 1+\delta$ or $r_k(t_1)^2 = 1-\delta$ for $k \in \mathbb{I}_{\mathrm{hit}}$, while $|r_i(t_1)^2 - 1| < \delta$ for $i \in \mathbb{I}_n \backslash \mathbb{I}_{\mathrm{hit}}$. When $r_k(t_1)^2 = 1+\delta$, using (19), the derivative of $r_k(t)^2/2$ at $t = t_1$ is given by

$$\frac{d}{dt}\left(\frac{r_k^2}{2}\right) = r_k \dot{r}_k = (1 - r_k^2) r_k^2 + \varepsilon r_k \alpha^{\mathsf{T}} r = -\delta(1+\delta) + \varepsilon r_k \alpha^{\mathsf{T}} r,$$

for some vector $\alpha \in \mathbb{R}^n$ dependent on H and $\theta(t_1)$. Since $|r_k \alpha^{\mathsf{T}} r|$ is bounded by a number that depends only on H and δ, the second term can be made smaller in magnitude than the first term by a choice of ε. Thus the derivative is negative, and r_k^2 decreases from $1+\delta$. By a similar argument, we see that the value of r_k^2 increases when $r_k(t_1)^2 = 1-\delta$. Hence, x cannot go across the boundary of $\mathbb{S}_\delta$, proving the invariance.

To show that $\mathbb{S}_\delta$ is locally attractive, suppose $x(t)$ is outside, but not too far from, the boundary of $\mathbb{S}_\delta$. That is, there exist $\rho \in \mathbb{R}$ and a subset of $\mathbb{I}_n$, denoted by $\mathbb{I}_{\mathrm{out}}$, such that $\delta \leq |r_k(t)^2 - 1| < \rho < 1/2$ for $k \in \mathbb{I}_{\mathrm{out}}$. The derivative of $r_k(t)^2/2$ is then bounded by

$$\begin{aligned} (d/dt)(r_k^2/2) &\leq -\delta(1+\delta) + \varepsilon r_k \alpha^{\mathsf{T}} r \ \text{ if } \ 1+\delta \leq r_k(t)^2 < 1+\rho, \\ (d/dt)(r_k^2/2) &\geq \ \ \delta(1-\delta) + \varepsilon r_k \alpha^{\mathsf{T}} r \ \text{ if } \ 1-\rho < r_k(t)^2 \leq 1-\delta. \end{aligned}$$

Following a similar argument as before, for a small enough choice of ε, the bound on the derivative is sign definite until $r_k(t)$ hits the boundary of $\mathbb{S}_\delta$ to take value $1+\delta$ or $1-\delta$. Thus, x will enter $\mathbb{S}_\delta$.

Proof of Lemma 2:

Proof First note from (8) that

$$\lambda = \sup \mu \qquad \text{such that} \qquad \lim_{t\to\infty} e^{-2\mu t}||\Phi(t)||^2 \to \infty.$$

Based on matrix norm properties, the following inequalities hold:

$$||\Phi(t)||^2 \geq \frac{1}{2n}||\Phi(t)||_F^2 \geq \frac{1}{2n\|P(t)\|}\mathrm{tr}(\Phi(t)^\intercal P(t)\Phi(t)) \geq \frac{\varsigma}{2n}\rho(t),$$

where $\|\cdot\|_F$ is the Frobenius norm, and ς is a constant defined such that $||P(t)|| < 1/\varsigma$ for all $t \geq 0$. Let $\tilde{\mu}_\delta \triangleq \tilde{\mu} - \delta$ for sufficiently small $\delta > 0$. Then

$$\lim_{t\to\infty} e^{-2\tilde{\mu}_\delta t}||\Phi(t)||^2 \geq \lim_{t\to\infty}\frac{\varsigma}{2n}e^{-2\tilde{\mu}_\delta t}\rho(t) \to \infty.$$

Since $\tilde{\mu}_\delta$ can make the left hand side go to infinity, we conclude that $\lambda \geq \tilde{\mu}$.

Proof of Lemma 5:

Proof By Lemma 4, all possible harmonic solutions have the form (14). Substituting $\xi(t)$ into (3) gives

$$(\mathcal{M}(\omega,\gamma) + \varepsilon H)\xi(t) = 0, \qquad \mathcal{M}(\omega,\gamma) := \begin{bmatrix} I - \Gamma^2 & -I + \mathcal{W} \\ I - \mathcal{W} & I - \Gamma^2 \end{bmatrix}$$

where $\mathcal{W}$ and Γ denote diagonal matrices of ω and γ, respectively. Noting that

$$\int_0^{2\pi/\omega} \xi(t)\xi(t)^\intercal dt = \frac{1}{2}\Omega_\varphi V V^\intercal \Omega_\varphi^\intercal, \qquad V := \begin{bmatrix} \gamma & 0 \\ 0 & \gamma \end{bmatrix},$$

we see that $\xi(t)$ is a solution of the dynamical system if and only if

$$(\mathcal{M}(\omega,\gamma) + \varepsilon H)\,\Omega_\varphi V = 0.$$

This equation is further equivalent to

$$(\Gamma^2 - I)\gamma = \varepsilon\bar{H}_{11}\gamma = \varepsilon\bar{H}_{22}\gamma, \qquad (\mathcal{W} - I)\gamma = \varepsilon\bar{H}_{21}\gamma = -\varepsilon\bar{H}_{12}\gamma,$$

where we noted that $\mathcal{M}(\omega,\gamma)$ and Ω_φ commute. The structure of H in (12) implies $\bar{H}_{11} = \bar{H}_{22}$ and $\bar{H}_{12} = -\bar{H}_{21}$, and hence the second and fourth equalities are satisfied. The first equality is expressed as

$$\eta(\varepsilon,\gamma) := (\Gamma^2 - I)\gamma - \varepsilon\bar{H}_{11}\gamma = 0.$$

Clearly, γ_i satisfying this condition for a small $|\varepsilon|$ has to be close to 1, -1, or 0. All the harmonic solutions near $|\gamma| = \mathring{\mathbf{1}}$ can be captured by those near $\gamma = \mathring{\mathbf{1}}$ due to the freedom in φ. By the implicit function theorem, $\eta(\varepsilon,\gamma) = 0$ is solvable for γ when $|\varepsilon|$ is sufficiently small since $\eta(0,\mathring{\mathbf{1}}) = 0$ and $\partial\eta/\partial\gamma(0,\mathring{\mathbf{1}}) = 2I$ hold. In particular, the solution in the neighborhood of $\gamma = \mathring{\mathbf{1}}$ is expressed as $\gamma = g(\varepsilon)$ for a continuously differentiable function g such that $g(0) = \mathring{\mathbf{1}}$, and the derivative is given by

$$\frac{\partial g}{\partial \varepsilon}(0) = -\left(\frac{\partial \eta}{\partial \gamma}(0, \mathring{\mathbf{1}})\right)^{-1} \frac{\partial \eta}{\partial \varepsilon}(0, \mathring{\mathbf{1}}) = \frac{1}{2}\bar{H}_{11}\mathring{\mathbf{1}}.$$

The formula for γ now follows as the Taylor series and that for ω is then obtained by solving the third equality.

Acknowledgements This research was supported by the National Science Foundation (NSF) Graduate Research Fellowship under Grant No. DGE-1144087.

Compliance with ethical standard

Conflict of interest The authors declare that they have no conflict of interest.

References

1. N. Stergiou, L.M. Decker, Human Movement Science **30**(5), 869 (2011)
2. M. Rabinovich, H. Abarbanel, Neuroscience **87**(1), 5 (1998)
3. U.H. Buzzi, N. Stergiou, M.J. Kurz, P.A. Hageman, J. Heidel, Clinical Biomechanics **18**(5), 435 (2003)
4. F. Cignetti, F. Schena, A. Rouard, Journal of Biomechanics **42**(10), 1452 (2009)
5. M.J. Kurz, N. Stergiou, Biological Cybernetics **93**(3), 213 (2005)
6. A.J. Mandell, K.A. Selz, Journal of Statistical Physics **70**(1-2), 355 (1993)
7. T. Shinbrot, C. Grebogi, J.A. Yorke, E. Ott, nature **363**(6428), 411 (1993)
8. G. Chen, D. Lai, in *Decision and Control, 1997., Proceedings of the 36th IEEE Conference on*, vol. 1 (IEEE, 1997), vol. 1, pp. 367–372
9. G. Chen, D. Lai, International Journal of Bifurcation and Chaos **8**(07), 1585 (1998)
10. L. Yang, Z. Liu, G. Chen, International Journal of Bifurcation and chaos **12**(05), 1121 (2002)
11. Ö. Morgül, International Journal of Bifurcation and Chaos **13**(11), 3449 (2003)
12. O.V. Popovych, Y.L. Maistrenko, P.A. Tass, Physical Review E **71**(6), 065201 (2005)
13. X. Li, G. Chen, IEEE Transactions on Circuits and Systems I: Fundamental Theory and Applications **50**(11), 1381 (2003)
14. I.Z. Kiss, C.G. Rusin, H. Kori, J.L. Hudson, Science **316**(5833), 1886 (2007)
15. X.F. Wang, G. Chen, X. Yu, Chaos: An Interdisciplinary Journal of Nonlinear Science **10**(4), 771 (2000)
16. S. Yu, G. Chen, Communications in Nonlinear Science and Numerical Simulation **17**(6), 2617 (2012)
17. Y. Kuramoto, *Chemical oscillations, waves, and turbulence*, vol. 19 (Springer Science & Business Media, 2012)
18. N. Tukhlina, M. Rosenblum, A. Pikovsky, J. Kurths, Physical Review E **75**(1), 011918 (2007)
19. S. Kohannim, Optimal oscillations and chaos generation in biologically-inspired systems. Ph.D. thesis, UCLA (2016)
20. D.A. Russell, J.D. Hanson, E. Ott, Physical Review Letters **45**(14), 1175 (1980)
21. J.D. Farmer, E. Ott, J.A. Yorke, in *The Theory of Chaotic Attractors* (Springer, 1983), pp. 142–169
22. A.L. Fradkov, R.J. Evans, Annual Reviews in Control **29**(1), 33 (2005)
23. A.L. Fradkov, V.A. Yakubovich, Vestn. LGU, Ser. Mat., Mekh., Astron **6**, 101 (1979)
24. F.C. Moon, *Chaotic and Fractal Dynamics: Introduction for Applied Scientists and Engineers* (John Wiley & Sons, 2008)
25. A. Hodgkin, A. Huxley, J. Physiol. **117**(4), 500 (1952)